COMMUNICATIONS IN COMPUTATIONAL PHYSICS
Vol. **5**, No. 2-4, pp. 546-564

Commun. Comput. Phys.
February 2009

An hp Adaptive Uniaxial Perfectly Matched Layer Method for Helmholtz Scattering Problems

Zhiming Chen[1,*], Benqi Guo[2] and Yuanming Xiao[1]

[1] *Institute of Computational Mathematics, Academy of Mathematics and Systems Science, Chinese Academy of Sciences, Beijing 100080, China.*
[2] *Department of Mathematics, University of Manitoba, Winnipeg, MB R3T 2N2, Canada.*

Received 17 September 2007; Accepted (in revised version) 9 December 2007

Available online 1 August 2008

Abstract. We propose an adaptive strategy for solving high frequency Helmholtz scattering problems. The method is based on the uniaxial PML method to truncate the scattering problem which is defined in the unbounded domain into the bounded domain. The parameters in the uniaxial PML method are determined by sharp a posteriori error estimates developed by Chen and Wu [8]. An hp-adaptive finite element strategy is proposed to solve the uniaxial PML equation. Numerical experiments are included which indicate the desirable exponential decay property of the error.

AMS subject classifications: 65N30, 65N35, 65N50, 35J05

Key words: Adaptivity, uniaxial perfectly matched layer, time-harmonic scattering, Helmholtz equation, hp-finite element method.

1 Introduction

To numerically solve the scattering problem in an unbounded domain, the first problem to be settled is to truncate the computational domain without introducing excessive error into the computed solution. Two basic approaches have been developed for this goal, the perfectly matched layer (PML) and radiation boundary conditions, of which we choose the former one to formulate our problem.

Since Berenger [4] which proposed a PML technique for solving the time dependent Maxwell equations, various constructions of PML absorbing layers have been proposed and studied in the literature (cf., e.g., Turkel and Yefet [18], Teixeira and Chew [17]). The

*Corresponding author. *Email addresses:* zmchen@lsec.cc.ac.cn (Z. Chen), guo@cc.umanitoba.ca (B. Q. Guo), xym@lsec.cc.ac.cn (Y. M. Xiao)

basic idea of the PML technique is to surround the computational domain by a layer of finite thickness with specially designed model medium that would attenuate all the waves that propagate from inside the computational domain.

As the PML has to be truncated at a finite distance from the domain of interest, its external boundary produces artificial reflections. It is proved in Hohage et al. [13], Lassas and Somersalo [14] that the PML solution converges exponentially to the solution of the original scattering problem as the thickness of the PML layer tends to infinity. In practical applications involving PML techniques, one cannot afford to use a very thick PML layer if uniform finite element meshes are used due to excessive computational costs. On the other hand, a thin PML layer requires a rapid variation of the artificial material property which deteriorates the accuracy if too coarse mesh is used in the PML layer.

The adaptive PML technique was proposed in Chen and Wu [5] for a scattering problem by periodic structures (the grating problem), in Chen and Liu [6] for the acoustic scattering problem, and in Chen and Chen [7] for the Maxwell scattering problem. The main idea of the adaptive PML technique is to use the a posteriori error estimate to determine the PML parameters and to use the adaptive finite element method to solve the PML equations. The adaptive PML technique provides a complete numerical strategy to solve the scattering problems in the framework of finite element which produces automatically a coarse mesh size away from the fixed domain and thus makes the total computational costs insensitive to the thickness of the PML absorbing layer.

The uniaxial PML method is widely used in the engineering literature. It provides greater flexibility and efficiency to solve problems involving anisotropic scatterers as opposing to circular PML method. In Chen and Wu [8], the adaptive PML technique developed for circular PML methods in [5–7] is extended to the uniaxial PML methods and the convergence proof of the uniaxial PML method is given.

While the low-order adaptive method based on the uniaxial PML technique can save considerable computational costs, it still suffers from the drawback that the CPU time and memory storage grow rapidly as the accuracy requirement of the computed solution increases. Even for scatterers only a few wavelengths in size, the computer resources required may be excessive for computing far field patterns to a few digits of accuracy by low-order methods. One remedy is to use the hp version of the finite element which simultaneously refines the mesh and increases the degrees of elements uniformly or selectively. In contrast to the classical h version with low-order basis functions which yields algebraic decay of error in terms of the number of unknowns, the hp version enjoys the attractive feature of exponential rate of convergence with proper choices of meshes and element degrees (see, e.g., Babuška and Guo [2] for elliptic equations).

Our purpose in this paper is to recover this essential feature to achieve high accuracy of the hp FEM in the scattering problem with singular solutions, especially, for high wave numbers. Our hp-adaptive finite element strategy is based on the a posteriori error estimate developed by following the procedure of [8], of which the new ingredient is the dependence of the element degree in our local error estimator. We borrow the hp Clément interpolant in Melenk and Wohlmuth [10] to achieve this sharp hp error estimates.

The layout of this paper is as follows. In Section 2 we recall the classical two dimensional Helmholtz-type scattering problem and the boundary integral representation of the solution to the exterior Helmholtz equation. By using the method of the complex coordinate stretching in Chew and Weedon [20], we recall the uniaxial PML formulation. In Section 3, we introduce the finite element approximation. In Section 4, based on the error representation formula, we derive the a posteriori error estimate which includes both the PML error and the finite element discretization error. In Section 5 we give a complete description of our *hp* adaptive algorithm. Finally in Section 6 we present two examples to show the competitive behavior of the method.

2 The PML equation

Let the scatterer $D\subset\mathbb{R}^2$ be a bounded domain with Lipschitz boundary Γ_D, and $\mathbf{n}_D$ be the unit outer normal to Γ_D. Our aim is to solve the following Helmholtz-type scattering problems with perfectly conducting boundary:

$$\Delta u+k^2u=0 \quad \text{in } \mathbb{R}^2\backslash\bar{D}, \tag{2.1}$$

$$\frac{\partial u}{\partial \mathbf{n}_D}=-g \quad \text{on } \Gamma_D, \tag{2.2}$$

$$\sqrt{r}\left(\frac{\partial u}{\partial r}-\mathrm{i}ku\right)\to 0 \quad \text{as } r=|x|\to\infty. \tag{2.3}$$

Here $g\in H^{-1/2}(\Gamma_D)$ is determined by the incoming wave. We assume the wave number $k=\omega/c$ is a constant, with ω being the angular frequency of the waves and c the sound speed of the fluid in the background media.

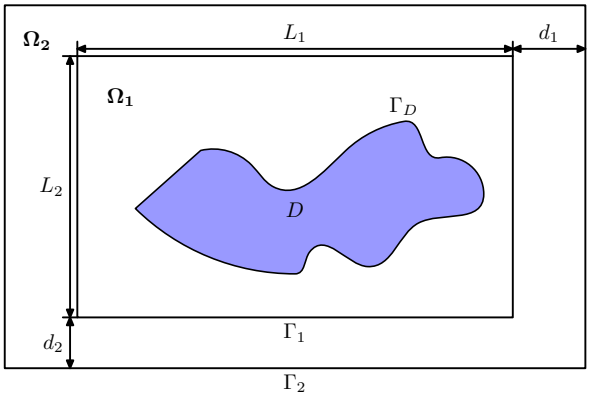

Figure 1: Setting of the scattering problem with the PML layer.

Let D be contained in the interior of the rectangle $B_1=\{x\in\mathbb{R}^2: |x_1|<L_1/2, |x_2|<L_2/2\}$. Let $\Gamma_1=\partial B_1$ and $\mathbf{n}_1$ the unit outer normal to Γ_1. We denote f and $Tf=\partial u/\partial\mathbf{n}_1$ the Dirichlet

and Neumann trace of u on Γ_1, respectively. By the third Green formula, the solution to the Helmholtz equation (2.1)-(2.3) satisfies

$$u=-\Psi_{SL}^k(Tf)+\Psi_{DL}^k(f) \quad \text{in } \mathbb{R}^2\backslash\bar{B}_1,$$

where Ψ_{SL}^k,Ψ_{DL}^k are respectively the single and double layer potentials

$$\Psi_{SL}^k(\lambda)(x)=\int_{\Gamma_1} G_k(x,y)\lambda(y)ds(y), \quad \forall\lambda\in H^{-1/2}(\Gamma_1),$$
$$\Psi_{DL}^k(g)(x)=\int_{\Gamma_1} \frac{\partial G_k(x,y)}{\partial \mathbf{n}_1(y)}g(y)ds(y), \quad \forall g\in H^{1/2}(\Gamma_1).$$

Here $G_k=\frac{\mathrm{i}}{4}H_0^{(1)}(k|x-y|)$ is the fundamental solution of the Helmholtz equation satisfying the Sommerfeld radiation condition, where $H_0^{(1)}(z)$ is the zeroth-order Hankel function of the first kind.

To introduce the absorbing PML layer, we use the notation in Fig. 1. Let $\Omega_1=B_1\backslash\bar{D}$ be the physical domain, i.e., the subdomain where we are interested in computing the solution of (2.1)-(2.3). Let

$$B_2=\{x\in\mathbb{R}^2:\ |x_1|<L_1/2+d_1,|x_2|<L_2/2+d_2\}$$

be the rectangle which contains B_1. Our PML equation is defined in the computational domain $\Omega_2=B_2\backslash\bar{D}$. The inner and outer boundary of the absorbing layer are denoted by Γ_1 and Γ_2, respectively.

We consider the anisotropic model medium property in the PML, with

$$\alpha_1(x_1)=1+\mathrm{i}\sigma_1(x_1), \quad \alpha_2(x_2)=1+\mathrm{i}\sigma_2(x_2),$$

applying to the vertical and horizontal layers, respectively. They satisfy

$$\sigma_j\in C(\mathbb{R}),\ \sigma_j\geq 0,\ \sigma_j(t)=\sigma_j(-t),\ \text{and}\ \ \sigma_j(t)=0\ \text{ for }\ |t|\leq L_j/2,\ j=1,2.$$

Furthermore, we make the following assumptions on the fictitious medium property, which is rather mild in the practical application of the uniaxial PML method

(H1) $\displaystyle\int_0^{\frac{L_1}{2}+d_1}\sigma_1(t)dt=\int_0^{\frac{L_2}{2}+d_2}\sigma_2(t)dt=\sigma,\ \sigma>0$ is a constant;

(H2) $\displaystyle\sigma_j(t)=\tilde{\sigma}_j\left(\frac{|t|-L_j/2}{d_j}\right)^m,\ m\geq 1$ integer, $\tilde{\sigma}_j>0$ is a constant, $j=1,2.$

We follow the method of complex coordinate stretching [20] to introduce the PML equation. Let $\tilde{x}_j$ denote the complex coordinate defined by

$$\tilde{x}_j=\begin{cases} x_j & \text{if } |x_j|<L_j/2,\\ \int_0^{x_j}\alpha_j(t)dt & \text{if } |x_j|\geq L_j/2.\end{cases}$$

For $z\in\mathbb{C}\backslash[0,+\infty)$, denote by $z^{1/2}$ as the analytic branch of $\sqrt{z}$ with $\mathrm{Im}(z^{1/2})>0$. Let

$$\rho(\tilde{x},y)=[(\tilde{x}_1-y_1)^2+(\tilde{x}_2-y_2)^2]^{1/2}$$

be the complex distance. As previous, we denote f the Dirichlet trace of u on Γ_1, and define

$$\tilde{G}_k(x,y)=\frac{\mathrm{i}}{4}H_0^{(1)}(k\rho(\tilde{x},y)).$$

The PML extension of $u|_{\Gamma_1}$ outside B_1 thus can be introduced as follows

$$\tilde{u}(x)=-\tilde{\Psi}_{SL}^k(Tf)+\tilde{\Psi}_{DL}^k(f)\quad\text{in }\mathbb{R}^2\backslash\bar{B}_1.$$

Here $\tilde{\Psi}_{SL}^k,\tilde{\Psi}_{DL}^k$ are similar to Ψ_{SL}^k,Ψ_{DL}^k respectively, with the integral kernel $G_k(x,y)$ replaced by $\tilde{G}_k(x,y)$. It is obviously to see the PML extension satisfies

$$\frac{\partial^2\tilde{u}}{\partial\tilde{x}_1^2}+\frac{\partial^2\tilde{u}}{\partial\tilde{x}_2^2}+k^2\tilde{u}=0\quad\text{in }\mathbb{R}^2\backslash\bar{B}_1,$$

which yields the desired PML equation in Cartesian coordinates

$$\frac{\partial}{\partial x_1}\left(\frac{\alpha_2}{\alpha_1}\frac{\partial\tilde{u}}{\partial x_1}\right)+\frac{\partial}{\partial x_2}\left(\frac{\alpha_1}{\alpha_2}\frac{\partial\tilde{u}}{\partial x_2}\right)+\alpha_1\alpha_2k^2\tilde{u}=0\quad\text{in }\mathbb{R}^2\backslash\bar{B}_1.$$

Since

$$H_0^{(1)}(z)\sim\sqrt{\frac{2}{\pi z}}e^{\mathrm{i}\left(z-\frac{\pi}{4}\right)}\quad\text{as }|z|\to\infty,$$

it is easy to see $H_0^{(1)}(z)$ decays exponentially on the upper half complex plane. Heuristically, we expect $\tilde{u}(x)$ have the same property for x away from Γ_1. The PML problem is then to find $\hat{u}$, which approximates u in Ω_1

$$\nabla\cdot(A\nabla\hat{u})+\alpha_1\alpha_2k^2\hat{u}=0\quad\text{in }\Omega_2,\tag{2.4}$$

$$\frac{\partial\hat{u}}{\partial\mathbf{n}_D}=-g\ \text{ on }\Gamma_D,\quad\hat{u}=0\ \text{ on }\Gamma_2,\tag{2.5}$$

where

$$A=\mathrm{diag}(\alpha_2(x_2)/\alpha_1(x_1),\alpha_1(x_1)/\alpha_2(x_2))$$

is a diagonal matrix.

The well-posedness of the PML problem (2.4)-(2.5) as well as the convergence of its solution to that of the original scattering problem is studied in [8]. The main goal of the following sections is to develop an *hp* adaptive strategy to solve the truncated PML problems (2.4)-(2.5).

3 Finite element approximation

In this section we describe the precise assumptions on the underlying meshes and introduce the finite element approximation of the PML problems (2.4)-(2.5). Let $\mathcal{M}_h$ be a conforming regular triangulation of the domain Ω_2, i.e., it satisfies

1. (partition) The elements $K\in\mathcal{M}_h$ may have one curved edge align with Γ_D so that $\Omega_2=\bigcup_{K\in\mathcal{M}_h}K$.
2. (conformity) No vertex of any element lies in the interior of a side of another element.
3. (shape regularity) The ratio between the diameter of an element and that of its inscribed circle is bounded above by a constant independent of the triangulation.

In particular, the regularity assumption does not rule out locally refined meshes that arise in an adaptive refinement procedure.

For a mesh $\mathcal{M}_h$ of elements $K_j, 1\leq j\leq J$, and a distribution of polynomial degrees $\mathcal{P}=(p_1,p_2,\cdots,p_J)$, we construct a continuous finite element spaces

$$V_{hp}=V_{hp}(\mathcal{M}_h;\mathcal{P})$$

of which the restriction on each element K_j is a polynomial with the degree not exceeding p_j. Define

$$\overset{\circ}{V}_{hp}=\overset{\circ}{V}_{hp}(\mathcal{M}_h;\mathcal{P})=\{v\in V_{hp}:v=0 \text{ on } \Gamma_2\},$$

and $b:H^1(\Omega_2)\times H^1(\Omega_2)\to\mathbb{C}$ the sesquilinear form given by

$$b(\varphi,\psi)=\int_{\Omega_2}\left(A\nabla\varphi\cdot\nabla\bar{\psi}-\alpha_1\alpha_2k^2\varphi\bar{\psi}\right)dx. \tag{3.1}$$

Standard arguments in the finite element framework lead to the following discrete problem from the weak formulation of problem (2.4)-(2.5): Find $u_{hp}\in\overset{\circ}{V}_{hp}$ such that

$$b(u_{hp},\psi_{hp})=\int_{\Gamma_D}g\bar{\psi}_{hp}ds,\quad \forall\psi_{hp}\in\overset{\circ}{V}_{hp}. \tag{3.2}$$

4 A posteriori error estimates

Having the finite element approximation u_{hp} in hand, the central issue in the a posteriori error estimation is to find a quantitative representation of the true error $u-u_{hp}$ measured in a specified norm in terms of the Galerkin approximation u_{hp} and the boundary data g. In this section we will derive such an error representation formula.

For any $\varphi \in H^1(\Omega_1)$, let $\breve{\varphi}$ be its extension in $\Omega^{\text{PML}} = \Omega^2 \backslash \bar{\Omega}^1$ such that $\breve{\varphi}|_{\Omega^{\text{PML}}} = w$ satisfying

$$\nabla \cdot (A \nabla w) + \alpha_1 \alpha_2 k^2 w = 0 \quad \text{in } \Omega^{\text{PML}}, \tag{4.1}$$

$$w = \varphi \ \text{ on } \Gamma_1, \quad w = 0 \ \text{ on } \Gamma_2. \tag{4.2}$$

We define

$$\hat{T}\varphi = \partial w / \partial \mathbf{n}_1, \quad \tilde{\varphi} = \breve{\bar{\varphi}}.$$

Similar to (3.1), the sesquilinear form of the original Helmholtz problem is written as

$$a(\varphi, \psi) = \int_{\Omega_1} \left(\nabla \varphi \cdot \nabla \bar{\psi} - k^2 \varphi \bar{\psi} \right) dx - \int_{\Gamma_1} T\varphi \cdot \bar{\psi} ds. \tag{4.3}$$

The continuous weak formulation is, find $u \in H^1(\Omega_1)$ such that

$$a(u, \psi) = \int_{\Gamma_D} g \bar{\psi} ds, \quad \forall \psi \in H^1(\Omega_1).$$

The existence of a unique solution of the scattering problem is known (cf., e.g., [12], McLean [15]). Then the general theory in Babuška and Aziz [1, Chap. 5] implies that there exists a constant $\mu > 0$ such that the following inf-sup condition is satisfied

$$\sup_{0 \neq \psi \in H^1(\Omega_1)} \frac{|a(\varphi, \psi)|}{\|\psi\|_{H^1(\Omega_1)}} \geq \mu \|\varphi\|_{H^1(\Omega_1)}, \quad \forall \varphi \in H^1(\Omega_1). \tag{4.4}$$

By definition of (4.3), we have $\forall \varphi \in H^1(\Omega_1)$,

$$\begin{aligned} & a(u - u_{hp}, \varphi) \\ = & \int_{\Gamma_D} g \bar{\varphi} ds - \int_{\Omega_1} (A \nabla u_{hp} \cdot \nabla \bar{\varphi} - \alpha_1 \alpha_2 k^2 u_{hp} \bar{\varphi}) dx + \int_{\Gamma_1} T u_{hp} \cdot \bar{\varphi} ds \\ = & \int_{\Gamma_D} g \bar{\varphi} ds - b(u_{hp}, \tilde{\varphi}) + \int_{\Omega^{\text{PML}}} (A \nabla u_{hp} \cdot \nabla \tilde{\bar{\varphi}} - \alpha_1 \alpha_2 k^2 u_{hp} \tilde{\bar{\varphi}}) dx + \int_{\Gamma_1} T u_{hp} \cdot \bar{\varphi} ds. \end{aligned} \tag{4.5}$$

From the definition of $\tilde{\varphi}$, integrating by parts, we deduce that

$$\int_{\Omega^{\text{PML}}} (A \nabla \tilde{\bar{\varphi}} \cdot \nabla u_{hp} - \alpha_1 \alpha_2 k^2 \tilde{\bar{\varphi}} u_{hp}) dx = - \int_{\Gamma_1} T \tilde{\bar{\varphi}} \cdot u_{hp} ds.$$

On the other hand,

$$- \int_{\Gamma_1} T \tilde{\bar{\varphi}} \cdot u_{hp} ds = \int_{\Omega^{\text{PML}}} (A \nabla \tilde{\bar{\varphi}} \cdot \nabla \breve{u}_{hp} - \alpha_1 \alpha_2 k^2 \tilde{\bar{\varphi}} \breve{u}_{hp}) dx = - \int_{\Gamma_1} T \breve{u}_{hp} \cdot \bar{\varphi} ds.$$

Substituting above equation into (4.5) and using the discrete variational form (3.2), we obtain our error representation formula, that is, $\forall \varphi_{hp} \in \overset{\circ}{V}_{hp}$,

$$\begin{aligned} & a(u-u_{hp},\varphi) \\ &= \int_{\Gamma_D} g\bar{\varphi}ds - b(u_{hp},\tilde{\varphi}) + \int_{\Gamma_1} (Tu_h - \hat{T}u_h)\bar{\varphi}ds \\ &= \int_{\Gamma_D} g(\overline{\varphi-\varphi_{hp}})ds - b(u_{hp},\tilde{\varphi}-\tilde{\varphi}_{hp}) + \int_{\Gamma_1} (Tu_h - \hat{T}u_h)\bar{\varphi}ds. \end{aligned} \tag{4.6}$$

This formula is the start point of the following a posteriori error estimation which is the basis to design our adaptive strategy. In our adaptive strategy to be presented later in the paper, the PML parameter is determined a priori so that the corresponding error is much smaller than the *hp*-discretization errors could become. We remark that different PML parameters lead to different computational domains and different coefficients in the PML equation. Therefore, it is more advantageous to determine them a priori rather than adaptively based on the a posteriori error estimate.

For any $K \in \mathcal{M}_h$, we denote by h_K its diameter. Let $\mathcal{B}_h$ denote the set of all sides that do not lie on Γ_D and Γ_2. For any $e \in \mathcal{B}_h$, h_e stands for its length. For any $K \in \mathcal{M}_h$, we introduce the element residual:

$$R_K := \nabla \cdot (A\nabla u_{hp}|_K) + \alpha_1\alpha_2 k^2 u_{hp}|_K.$$

For any interior side $e \in \mathcal{B}_h$ which is the common side of K_1 and $K_2 \in \mathcal{M}_h$, we define the jump residual across e:

$$J_e := (A\nabla u_{hp}|_{K_1} - A\nabla u_{hp}|_{K_2}) \cdot \nu_e,$$

using the convention that the unit normal vector ν_e to e points from K_2 to K_1. If

$$e = \Gamma_D \cap \partial K$$

for some element $K \in \mathcal{M}_h$, then we define the jump residual

$$J_e := 2(\nabla u_{hp}|_K \cdot \mathbf{n}_D + g).$$

Let p_K, p_e be the polynomial degree of element K and edge e, respectively. Denote by η_K and $\mathcal{E}$ the local error indicator and the a posteriori error estimate

$$\eta_K = \left(\frac{h_K^2}{p_K^2} \|R_K\|^2_{L^2(K)} + \frac{1}{2} \sum_{e \subset \partial K} \frac{h_e}{p_e} \|J_e\|^2_{L^2(e)} \right)^{1/2}, \quad \mathcal{E} = \left\{ \sum_{K \in \mathcal{M}_h} \eta_K^2 \right\}^{1/2}. \tag{4.7}$$

By the argument in Theorem 2.2 of [10], for any $u \in H^1(\Omega_2)$ vanishing on Γ_2, an *hp* Clément type interpolant $Iu \in \overset{\circ}{V}_{hp}$ can be constructed which is stable in the energy norm,

that is, for any $K\in\mathcal{M}_h$ and $p_K\geq 1$, the following estimate holds with $C>0$ depending only on the minimum angle of $\mathcal{M}_h$

$$||u-Iu||_{L^2(K)}+\frac{h_K}{p_K}||\nabla(u-Iu)||_{L^2(K)}+\sum_{e\subset\partial K}\sqrt{\frac{h_e}{p_e}}||u-Iu||_{L^2(e)}\leq C\frac{h_K}{p_K}||\nabla u||_{L^2(\tilde{K})}. \tag{4.8}$$

Here $\tilde{K}=\omega_K^8$ is a local patch of elements, with

$$\omega_K^0:=\{\text{vertices of } K\},\quad \omega_K^j:=\cup\{\bar{K}'|K'\in\mathcal{M}_h \text{ and } \bar{K}'\cap\omega_K^{j-1}\neq\emptyset\}.$$

We remark here that for any $K\in\mathcal{M}_h$, the number of elements in $\tilde{K}$ is bounded from above since our triangulation is shape-regular.

Now we take $\tilde{\varphi}_{hp}=I\tilde{\varphi}$ in the error representation formula (4.6) to get

$$\begin{aligned} a(u-u_{hp},\varphi) &= \int_{\Gamma_D} g(\overline{\varphi-I\tilde{\varphi}})ds-b(u_{hp},\tilde{\varphi}-I\tilde{\varphi})+\int_{\Gamma_1}(Tu_h-\hat{T}u_h)\bar{\varphi}ds \\ &:= \mathrm{II}_1+\mathrm{II}_2+\mathrm{II}_3. \end{aligned} \tag{4.9}$$

We observe that, by integration by parts

$$\mathrm{II}_1+\mathrm{II}_2=\sum_{K\in\mathcal{M}_h}\left(\int_K R_K(\overline{\tilde{\varphi}-I\tilde{\varphi}})dx+\sum_{e\subset\partial K}\frac{1}{2}\int_e J_e(\overline{\tilde{\varphi}-I\tilde{\varphi}})ds\right).$$

Standard argument in the a posteriori error analysis using (4.8) implies

$$\begin{aligned} |\mathrm{II}_1+\mathrm{II}_2| &\leq C\sum_{K\in\mathcal{M}_h}\left(\frac{h_K^2}{p_K^2}\|R_K\|^2_{L^2(K)}+\frac{1}{2}\sum_{e\subset K}\frac{h_e}{p_e}\|J_e\|^2_{L^2(e)}\right)^{1/2}||\nabla\tilde{\varphi}||_{L^2(\tilde{K})} \\ &\leq C\left(\sum_{K\in\mathcal{M}_h}\eta_K^2\right)^{1/2}||\nabla\tilde{\varphi}||_{L^2(\Omega_2)}. \end{aligned}$$

Concerning the third term of (4.9), we resort to the following key estimate between the Dirichlet-to-Neumann operator for the original scattering problem T and the PML problem $\hat{T}$, which is established in [8], for any $f\in H^{1/2}(\Gamma_1)$,

$$\|Tf-\hat{T}f\|_{H^{-1/2}(\Gamma_1)}\leq C|\alpha_m|^3(1+kL)^4e^{-(\gamma k\sigma-1)}\|f\|_{H^{1/2}(\Gamma_1)}.$$

Here,

$$\gamma=\frac{\min(d_1,d_2)}{\sqrt{(L_1+d_1)^2+(L_2+d_2)^2}},\quad L=\max(L_1,L_2),\quad \alpha_m=\max_{x\in\Gamma_2}(\alpha_1(x_1),\alpha_2(x_2)).$$

Thus

$$|\mathrm{II}_3|\leq C|\alpha_m|^3(1+kL)^4e^{-(\gamma k\sigma-1)}\|u_{hp}\|_{H^{1/2}(\Gamma_1)}\|\varphi\|_{H^{1/2}(\Gamma_1)}.$$

Together with the stability estimates [8] for the Dirichlet problem of the PML equation in the layer,

$$\|\nabla\tilde{\varphi}\|_{L^2(\Omega^{\rm PML})}\leq C|\alpha_m|^2(1+kL)\|\varphi\|_{H^1(\Omega_1)},$$

and by the inf-sup condition (4.4), we finally get the a posteriori error estimate

$$\begin{aligned}\|u-u_{hp}\|_{H^1(\Omega_1)}&\leq C\sup_{0\neq\varphi\in H^1(\Omega_1)}\frac{|a(u-u_{hp},\varphi)|}{\|\varphi\|_{H^1(\Omega_1)}}\\&\leq C|\alpha_m|^2(1+kL)\left(\sum_{K\in\mathcal{M}_h}\eta_K^2\right)^{1/2}+C|\alpha_m|^3(1+kL)^4e^{-(\gamma k\sigma-1)}\|u_{hp}\|_{H^{1/2}(\Gamma_1)}.\end{aligned}\tag{4.10}$$

5 *hp* adaptive algorithm

In this section we propose our implementation of the *hp* adaptive method. Note that in the previous section the derived a posteriori error estimate (4.10) consists of two parts: the finite element discretization error and the PML error. First we determine the PML parameters a priori through the second term of (4.10). We choose L_1,L_2 such that $D\subset B_1$ and choose d_1,d_2 such that

$$\frac{d_1}{L_1}=\frac{d_2}{L_2}=\chi,\tag{5.1}$$

where χ is a constant. Then we choose χ and σ such that the exponentially decaying factor

$$\omega=e^{-(\gamma k\sigma-1)}=e^{-\left(\frac{\chi}{\chi+1}\frac{\min(L_1,L_2)}{\sqrt{L_1^2+L_2^2}}k\sigma-1\right)}\leq 10^{-8},$$

which makes the PML error negligible compared with the finite element discretization errors. By **(H2)**,

$$\sigma_j(t)=\tilde{\sigma}_j\left(\frac{|t|-L_j/2}{d_j}\right)^m,\quad j=1,2,$$

where $\tilde{\sigma}_1,\tilde{\sigma}_2$ are determined from σ as follows

$$\tilde{\sigma}_j=(m+1)\sigma/d_j,\quad j=1,2.\tag{5.2}$$

Once the PML region and the medium property are fixed, we use the standard finite element adaptive strategy to modify the mesh according to the a posteriori error estimate. Now we present our *hp* adaptive algorithm as follows:

Algorithm 5.1:

Given tolerance TOL >0. Let $m=2$ and n_h the times of h-refinement on the mesh $\mathcal{M}_h$ associated with degree distribution $\mathcal{P}$ before performing p-refinement. In practice, we choose n_h=2 or 3.

- Choose L_1,L_2 such that $D\subset B_1$;
- Choose χ and σ such that the exponentially decaying factor $\omega\leq 10^{-8}$;
- Set d_1,d_2 and $\tilde{\sigma}_1$,$\tilde{\sigma}_2$ according to (5.1) and (5.2);
- Generate an initial mesh $\mathcal{M}_h^{(1)}$ over $\Omega_2=B_2\backslash\bar{D}$ and select the initial element degree distribution $\mathcal{P}^{(1)}=1$;
- Compute finite element solution $u_1\in\overset{\circ}{V}_{hp}(\mathcal{M}_h^{(1)};\mathcal{P}^{(1)})$;
- Compute error indicators η_K,$K\in\mathcal{M}_h^{(1)}$ for $u_1\in\overset{\circ}{V}_{hp}(\mathcal{M}_h^{(1)};\mathcal{P}^{(1)})$;
- Set initial $n=0$,$k=1$;
- While

$$\mathcal{E}_k=\left(\sum_{K\in\mathcal{M}_h^{(k)}}\eta_K^2\right)^{1/2}>\text{TOL},\tag{5.3}$$

do

If $n<n_h$, perform h-refinement:

- Refine all $K\in\mathcal{M}_h^{(k)}$ satisfying $\eta_K>\frac{1}{2}\max(\eta_K,K\in\mathcal{M}_h^{(k)})$ to construct a conforming mesh $\mathcal{M}_h^{(k+1)}$,
- Set the degree of newly generated element same as that of its parent and leave others unchanged. Denote the new distribution of element degree by $\mathcal{P}^{(k+1)}$,
- Set $n=n+1$,

Else, perform p-refinement:

- Set $p_j=p_j+1$ for each element K_j and let $\mathcal{M}_h^{(k+1)}=\mathcal{M}_h^{(k)}$,
- Set $n=0$,

Compute the finite element solution u_{k+1} in the new finite element space $\overset{\circ}{V}_{hp}(\mathcal{M}_h^{(k+1)};\mathcal{P}^{(k+1)})$ and the error indicators η_{K_j},$K_j\in\mathcal{M}_h^{(k+1)}$.

Set $k=k+1$,

End while

The guideline of the hp adaptive algorithm is to achieve the error equi-distribution on the elements by using either h-refinement or p-refinement. It is well-known that the h-refinement is preferred around the singularity of the solution and the p-refinement is preferred in the region where the solution is smooth. In our algorithm we use the finite element method of a uniform degree on the mesh. The degree of the finite elements is successively increased only after $n_h=2$,or 3 number of h-refinements is performed. The h-refinement is governed by the usual adaptive strategy based on the sharp a posteriori error indicator which captures the singularity of the solution. We find that this simple hp adaptive strategy can already achieve the desired exponential convergence of the error in terms of the number of degree of freedoms.

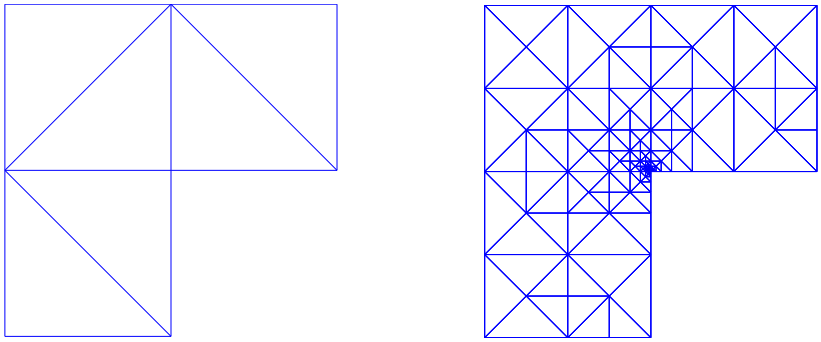

(a) Initial mesh $\mathcal{M}_h^{(1)}$ with $\mathcal{P}^{(1)}$ (b) A refined mesh $\mathcal{M}_h$ with $\mathcal{P}^{(3)}=3$

Figure 2: The initial mesh and the refined mesh.

6 Numerical results

In this section, we provide three numerical examples to demonstrate the efficiency of the proposed algorithm.

6.1 Poisson's equation

In this example, we solve an elliptic equation defined in an L-shaped domain to test whether our algorithm can produce quasi-optimal meshes. The weak formulation is to find $u\in H_0^1(\Omega)$, such that

$$\int_\Omega \nabla u\cdot\nabla v dx=\int_\Omega fv dx \quad \forall v\in H_0^1(\Omega).$$

The local hp-indicator becomes

$$\eta_K^2:=\frac{h_K^2}{p_K^2}\|f+\Delta u_{hp}\|_{L^2(K)}^2+\sum_{e\in\partial K}\frac{h_e}{2p_e}\|J_e\|_{L^2(e)}^2.$$

Here,

$$J_e:=(\nabla u_{hp}|_{K_1}-\nabla u_{hp}|_{K_2})\cdot\nu_e.$$

The exact solution is $u=r^{\frac{2}{3}}\sin(\frac{2}{3}\theta)(x^2-1)(y^2-1)$, which is singular at the origin. Fig. 2 gives the initial mesh and an adaptively refined mesh after 6 steps.

It is well known that with properly designed geometric meshes, the hp-FEM exhibits exponential rate of convergence for elliptic problems (cf., e.g., [2,9]). From the curve plots of errors and estimators on successive refined meshes (Fig. 3), we can easily see our adaptive algorithm realizes the exponential convergence. More precisely, the discretization error in terms of the energy norm, as well as the a posteriori error estimate, is asymptotically proportional to $e^{-bN^{1/3}}$, where N denotes the number of degrees of freedom.

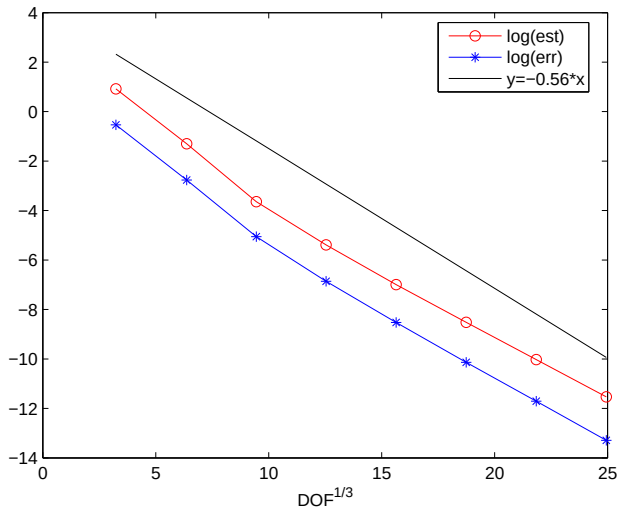

Figure 3: The exponential convergence of $\|u-u_k\|_{H^1(\Omega)}$ and the a posteriori error estimate $\mathcal{E}_k$ of (5.3).

Table 1: Performance of the hp adaptive finite element solution and the error estimator $\mathcal{E}_k$ of the form (5.3) (Example 1).

polynomial degree	degrees of freedom	number of elements	$\|u-u_k\|_{H^1(\Omega)}$	$\mathcal{E}_k/\|u-u_k\|_{H^1(\Omega)}$
1	34	50	5.8723e-01	4.2724
2	259	118	6.2785e-02	4.3364
3	844	178	6.3797e-03	4.0987
4	1,973	238	1.0477e-03	4.3716
5	3,826	298	1.9904e-04	4.5965
6	6,583	358	3.9662e-05	5.0434
7	10,424	418	8.2094e-06	5.3883
8	15,529	478	1.6864e-06	5.8221

Numerical results in Table 1 show that the effectivity index $\mathcal{E}_k/\|u-u_k\|_{H^1(\Omega)}$ is insensitive to h or p. Therefore the a posteriori error estimators are reliable and give precisely the distribution of the error in adaptive hp solution $u_k \in \overset{\circ}{V}_{hp}(\mathcal{M}_h^{(k)};\mathcal{P}^{(k)}), 1 \le k \le 8$.

6.2 The scattering problem with exact solutions

We consider the scattering problem whose exact solution is known: $u=H_0^{(1)}(k|x|)$. Let the scatterer $D=[-1,1]\times[-1,1]$. Equivalently, with respect to the wavelength $\lambda=2\pi/k$, the size of D is $\frac{k}{\pi}\lambda\times\frac{k}{\pi}\lambda$. We note that the scattered wave oscillates rapidly along the radial direction as the wave number gets high. It is essential to obtain some robust estimates

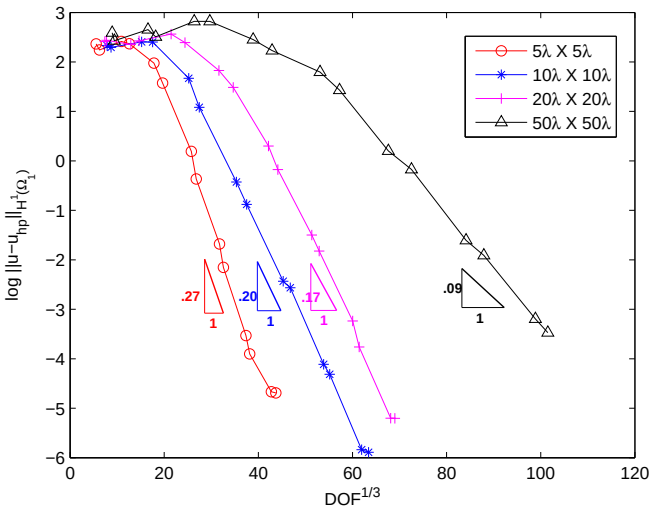

Figure 4: The exponential convergence of the hp adaptive solution for the group **(a)** (Example 2).

of the accuracy of a computed solution. Otherwise, the numerical outcome would be of limited usage.

Through this example we want to show that our hp a posteriori error estimate really give a measure of the discretization error. Furthermore, the exponential rate of convergence can be achieved by our algorithm. In particular, the error in the domain of interest

$$\|u-u_{hp}\|_{H^1(\Omega_1)} \approx Ce^{-bN^{1/3}}$$

asymptotically, where N denotes the number of degrees of freedom.

We have tested following wave numbers with specific given data:

(a) For $k=5\pi,10\pi,20\pi,50\pi$, choose $\chi=1.0$ and $L_1=L_2=2+8\pi/k$, that is, the width of the physical region is 2 times of wavelength. In order to make $\omega\leq 10^{-8}$, we choose $\sigma=54.93/k$.

(b) For $k=100\pi,200\pi,400\pi,600\pi$, choose $\chi=0.5$ and $L_1=L_2=2+40\pi/k$, that is, the width of the physical region is 10 times of wavelength. In order to make $\omega\leq 10^{-8}$, we choose $\sigma=82.40/k$.

Fig. 4 demonstrates the curves of $\log\|u-u_k\|_{H^1(\Omega_1)}$ with respect to $N_k^{1/3}$, where N_k is the number of unknowns of the finite element spaces $\overset{\circ}{V}_{hp}(\mathcal{M}_h^{(k)};\mathcal{P}^{(k)}),1\leq k\leq 8$, $u_k\in\overset{\circ}{V}_{hp}(\mathcal{M}_h^{(k)};\mathcal{P}^{(k)})$ is the hp finite element solution of (3.2). It indicates that the associated numerical complexity is quasi-optimal:

$$\|u-u_k\|_{H^1(\Omega_1)} \approx Ce^{-bN_k^{1/3}}$$

asymptotically, while different cases are related to different coefficients b and C. Although the exponential convergence is shown in Fig. 4 only for group **(a)**, it is also valid

Table 2: Performance of the hp adaptive solutions and the a posteriori error estimate $\mathcal{E}_k$ for the group **(b)** (Example 2).

wave number	scatterer size	degrees of freedom	polynomial degree	$\mathcal{E}_k/\|u-u_k\|_{H^1(\Omega)}$	relative error of far fields
100π	$100\lambda\times100\lambda$	1,178,755	5	11.854	6.91508e-04
200π	$200\lambda\times200\lambda$	1,961,967	7	9.3031	1.18274e-03
400π	$400\lambda\times400\lambda$	4,354,798	6	4.3181	7.07794e-03
600π	$600\lambda\times600\lambda$	7,238,844	8	3.5868	3.78647e-02

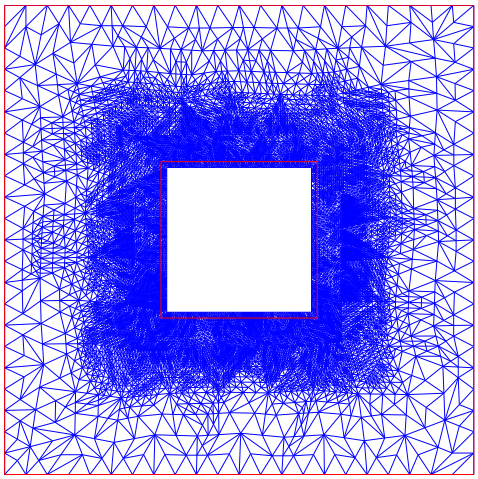

Figure 5: The mesh of 32,645 elements and polynomial degree of 8 for which DOFs $N=1{,}046{,}340$. The scatterer size is $50\lambda\times50\lambda$, $\chi=1.0$, $\sigma=0.35$ (Example 2).

for other choices of wave number and thickness of the PML layer.

Numerical results given in Table 2 show that our error estimates provide actual control of errors in energy norm.

One of the important quantities in the scattering problems is the far field pattern:

$$u_\infty(\hat{x})=\frac{e^{\mathrm{i}\frac{\pi}{4}}}{\sqrt{8\pi k}}\int_{\partial D}\left(u(y)\frac{\partial e^{-\mathrm{i}k\hat{x}\cdot y}}{\partial v(y)}-\frac{\partial u(y)}{\partial v(y)}e^{-\mathrm{i}k\hat{x}\cdot y}\right)ds(y),\quad \hat{x}=\frac{x}{|x|}.$$

For the special solution $u=H_0^{(1)}(k|x|)$, u_∞ has a simple expression $u_\infty=-\sqrt{2}\mathrm{i}e^{\mathrm{i}\frac{\pi}{4}}/\sqrt{k\pi}$, which is independent of the observation direction $\hat{x}$. As given in Table 2, for each case in group **(b)** where the wave number is fairly large, a relative error below 5% can be achieved with reasonable computational costs.

In Fig. 5 we show the mesh after 16 adaptive iterations when $k=50\pi$ and $\chi=1.0$. As expected, the mesh near the outer boundary Γ_2 is rather coarse since the PML solution decays quickly in the absorbing layer.

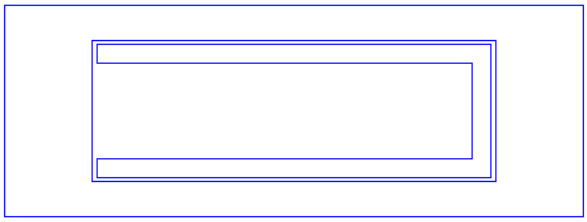

Figure 6: The configuration of the scatterer and the PML layer (Example 3).

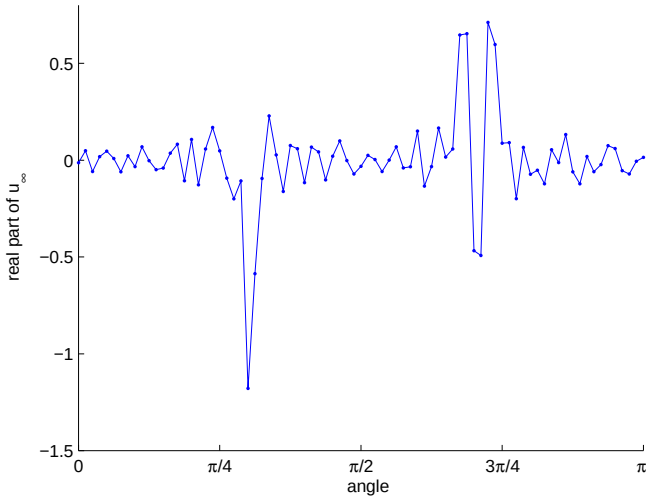

Figure 7: The real part of the far-field patterns calculated in the last adaptive step (124,499 elements, $p=8$, DOFs=3,991,812). The scatterer size is $210\lambda\times 70\lambda$, $\chi=d_j/L_j=0.2$, $\sigma=1.02$ (Example 3).

6.3 The scattering by the plane wave

In this example we compute the field scattered from a perfectly conducting metal by the plane wave $u_I=e^{ik\hat{p}x}$, $\hat{p}=(0.6,0.8)$. The scatterer is contained in the box $-2.1<x_1<2.1$ and $-0.7<x_2<0.7$, as shown in Fig. 6. In this example, the solution of the original scattering problem is no longer smooth due to the rough surface of the scatterer.

We test our algorithm when $k=100\pi$ and 200π, which corresponds to a scatterer of $210\lambda\times 70\lambda$ and $420\lambda\times 140\lambda$ in size, respectively. The minimum distance between the scatterer to the inner boundary Γ_1 is chosen to be 10 times of wavelength. In both cases we set $\chi=0.2$. To make $\omega\leq 10^{-8}$, we choose $\sigma=1.02$ for $k=100\pi$ and $\sigma=0.55$ for $k=200\pi$.

Fig. 7 demonstrates the real part of the far-field patterns calculated in the last adaptive step for $k=100\pi$. Fig. 8 shows the far fields calculated in the successive adaptive steps for the direction $\theta=\pi/4$ and $\theta=3\pi/4$. We observe that the calculated values of far fields become stable for the last several steps.

For non-smooth solution, our algorithm also enjoys the exponential convergence of

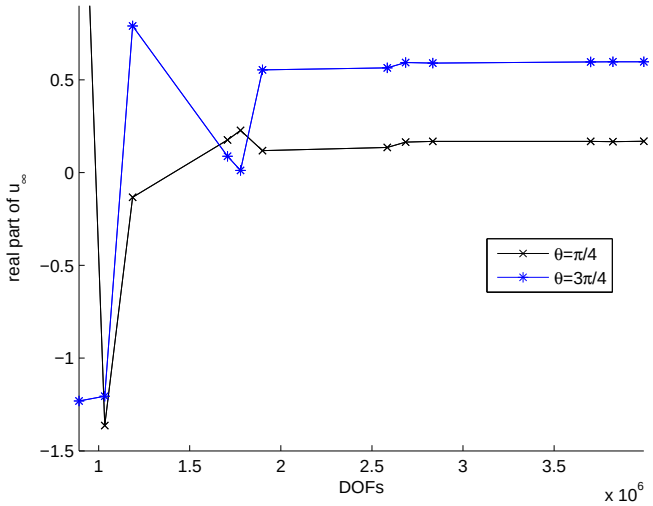

Figure 8: The real part of the far-field patterns when the observing angle $\theta=\pi/4$ and $\theta=3\pi/4$. The scatterer size is $210\lambda\times 70\lambda$, $\chi=d_j/L_j=0.2$, $\sigma=1.02$ (Example 3).

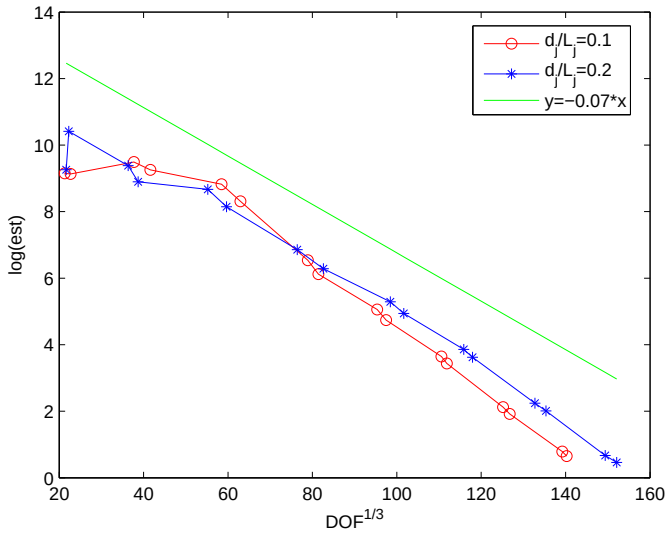

Figure 9: The quasi-optimality with different thickness of the PML layers. The scatterer size is $210\lambda\times 70\lambda$ (Example 3).

the hp-FEM solutions as well as the a posteriori error estimate $\mathcal{E}_k$ of the form (5.3). With fixed wave number $k=100\pi$, we test the influence of different thickness of PML layer. Fig. 9 shows that the exponential convergence is achieved in both cases.

In Fig. 10 we show the mesh after 22 adaptive steps when $k=200\pi$ and $\chi=0.2$. This again demonstrates one of advantages of the adaptive algorithm: it automatically determines where to refine the mesh and leave unchanged where the solution is smooth. For

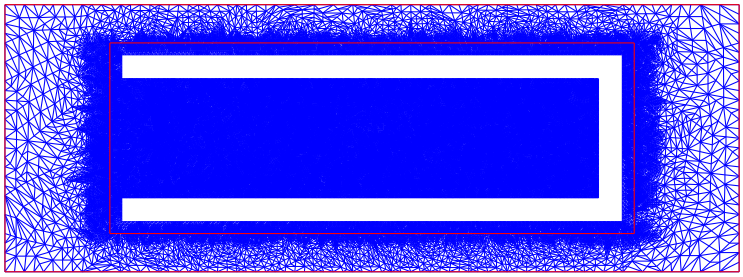

Figure 10: The mesh of 180,415 elements, 5,782,428 DOFs with polynomial degree of 8. The scatterer size is $420\lambda\times140\lambda$, $\chi=d_j/L_j=0.2$, $\sigma=0.55$ (Example 3).

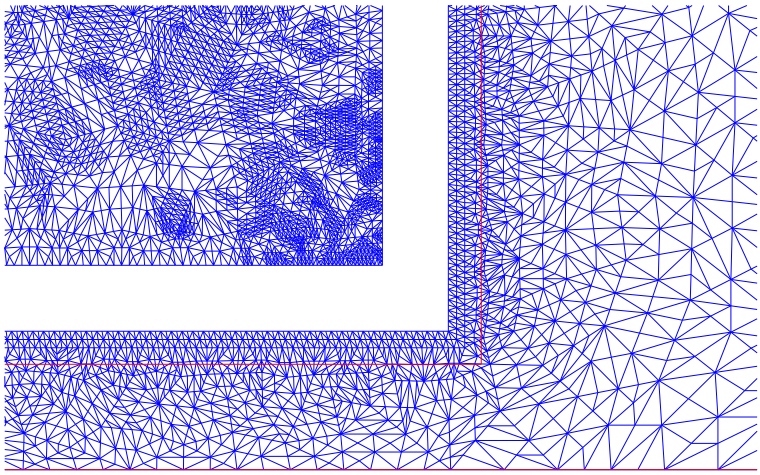

Figure 11: The mesh of 25,919 elements, 118,575 DOFs with polynomial degree of 3 (zoom in around the lower right corner). The scatterer size is $420\lambda\times140\lambda$, $\chi=d_j/L_j=0.2$, $\sigma=0.55$ (Example 3).

the PML formulation, this means we can choose a thick PML layer without making the computational costs too expensive. Fig. 11 shows part of the mesh zoomed around the lower right angle after 7 adaptive steps. One observes that the mesh is locally refined around the corner where the solution is singular.

Acknowledgments

The authors would like to thank the referees for their constructive comments that improved the presentation of the paper.

References

[1] I. Babuška and A. Aziz. *Survey Lectures on Mathematical Foundations of the Finite Element Method.* in The Mathematical Foundations of the Finite Element Method with Application to

Partial Differential Equations, ed. by A. Aziz, Academic Press, New York, 1973, 5-359.
[2] I. Babuška and B.Q. Guo. The *h-p* version of the finite element method for domains with curved boundaries. *SIAM J. Numer. Anal.*, 25 (1988), 837-861.
[3] I. Babuška and C. Rheinboldt. Error estimates for adaptive finite element computations. *SIAM J. Numer. Anal.*, 15 (1978), 736-754.
[4] J.-P. Berenger. A perfectly matched layer for the absorption of electromagnetic waves. *J. Comput. Phys.*, 114 (1994), 185-200.
[5] Z. Chen and H. Wu. An adaptive finite element method with perfectly matched absorbing layers for the wave scattering by periodic structures. *SIAM J. Numer. Anal.*, 41 (2003), 799-826.
[6] Z. Chen and X. Liu. An adaptive perfectly matched layer technique for time-harmonic scattering problems. *SIAM J. Numer. Anal.*, 43 (2005), 645-671.
[7] J. Chen and Z. Chen. An adaptive perfectly matched layer technique for 3-D time-harmonic electromagnetic scattering problems. *Math. Comp*, to apper.
[8] Z. Chen and X. Wu. An adaptive uniaxial perfectly matched layer method for time-harmornic scattering problems. *Numer. Math. Theor. Meth. Appl.*, 1 (2008), 113-137.
[9] B.Q. Guo. and I. Babuška. The *h-p* version of the finite element method, Part 1: The Basic Approximation Results; and Part 2: The General Results and Application, *Comp. Mech.*, 1 (1986), 22-41, and 203-220.
[10] J.M. Melenk and B.I. Wohlmuth. On residual-based a posteriori error estimation in hp-FEM. *Adv. Comput. Math.*, 15 (2001), 311-331.
[11] F. Collino and P.B. Monk. The perfectly matched layer in curvilinear coordinates. *SIAM J. Sci. Comput.*, 19 (1998), 2061-2090.
[12] D. Colton and R. Kress. *Integral Equation Methods in Scattering Theory.* John Wiley & Sons, New York, 1983.
[13] T. Hohage, F. Schmidt and L. Zschiedrich. Solving time-harmonic scattering problems based on the pole condition. II: Convergence of the PML method. *SIAM J. Math. Anal.*, 35 (2003), 547-560.
[14] M. Lassas and E. Somersalo. On the existence and convergence of the solution of PML equations. *Computing*, 60 (1998), 229-241.
[15] W. McLean. *Strongly Elliptic Systems and Boundary Integral Equations.* Cambridge University Press, Cambridge, 2000.
[16] CH. Schwab. *p- and hp-Finite Element Methods.* Clarendon Press, Oxford, 1998.
[17] F.L. Teixeira and W.C. Chew. Advances in the theory of perfectly matched layers. In: W.C. Chew et al, (eds.), Fast and Efficient Algorithms in Computational Electromagnetics, pp. 283-346, Artech House, Boston, 2001.
[18] E. Turkel and A. Yefet. Absorbing PML boundary layers for wave-like equations. *Appl. Numer. Math.*, 27 (1998), 533-557.
[19] G.N. Watson. *A Treatise on The Theory of Bessel Functions.* Cambridge, 1922.
[20] W. C. Chew and W. Weedon. A 3D perfectly matched medium from modified Maxwell's equations with stretched coordinates. *Microwave Opt. Tech. Lett.*, 7 (1994), 599-604.
[21] A. Schmidt and K. G. Siebert. *Design of Adaptive Finite Element Software: The Finite Element Toolbox ALBERTA.* Springer, 2005.